ISSN 0018-151X, High Temperature, 2017, Vol. 55, No. 3, pp. 380–385. © Pleiades Publishing, Ltd., 2017.
Original Russian Text © A.L. Smirnov, S.G. Taluts, A.D. Ivliev, V.I. Gorbatov, V.F. Polev, I.G. Korshunov, 2017, published in Teplofizika Vysokikh Temperatur, 2017, Vol. 55, No. 3, pp. 396–401.

THERMOPHYSICAL PROPERTIES OF MATERIALS

Thermal Diffusivity of Zirconium–Niobium Alloys at High Temperatures

A. L. Smirnov[a], *, S. G. Taluts[a], A. D. Ivliev[b], V. I. Gorbatov[a], V. F. Polev[a], and I. G. Korshunov[a, c]

[a] *Ural State Mining University, Ekaterinburg 620144, Russia*
[b] *Russian State Vocational Pedagogical University, Ekaterinburg 620012, Russia*
[c] *Institute of Thermal Physics, Ural Branch of RAS, Ekaterinburg, 620016, Russia*
**e-mail: ek-smirnov@yandex.ru*

Received May 25, 2015

Abstract—Experimental results are presented on the temperature-concentration dependences of thermal diffusivity, specific electrical resistivity, and thermal conductivity of zirconium-niobium alloys at high temperatures.

DOI: 10.1134/S0018151X17020183

INTRODUCTION

More than 90% of zirconium and its alloys produced all over the world are applied in nuclear power engineering as construction materials used to produce cartridge element**s,** cases, and other details of heat-generating cartridges, and channel tubes for thermal reactors [1]. In spite of that wide application, the kinetic properties of those materials at high temperatures are as a rule investigated for pure components as well as for several alloys and compositions most important in practice (e.g., [2–4]). Systematic study of the whole system properties was not performed earlier.

The present work is aimed at studying basic patterns of thermal diffusivity variation of the Zr–Nb alloys within the temperature range from 900 K to 1700 K. To interpret the obtained results, we also measure the specific electrical resistivity.

CHARACTERISTICS OF SPECIMEN AND EXPERIMENTAL TECHNIQUE

To prepare the specimens, we applied the NbSh 00 sort niobium and the zirconium iodide. We performed the alloys in the vacuum arc oven with a nonconsumable tungsten electrode in the helium atmosphere. To improve homogenization at the smelting, we performed thrice-repeated remelt with subsequent pouring into the copper mold, 12 mm in diameter. The oxygen admixture concentration was within 0.01%; carbon – within 0.03%; and nitrogen – 0.04%. The studied specimen composition is presented in the table. All the investigated materials were produced in the Laboratory for Precision Alloys and Intermetallides, Institute of Metal Physics, Ural Branch, RAS, Ekaterinburg.

We cut the specimens for the measurements by means of the electric-spark technique, with constant oil cooling, from one sort and one fusing ingots.

We performed the high-temperature thermal diffusivity measurements by the dynamic method of flat temperature waves by means of the automated measuring system described in [5, 6]. The measurements were done in vacuum of 10^{-3} Pa. We produced the temperature wave in the studied specimen via impact by the amplitude-modulated flow of electrons. The studied specimen served the anode of the vacuum diode. The temperature wave frequencies (the frequencies of modulation of the electron flow) were equal 5–30 Hz. We determined the averaged (over the modulation period) temperature by means of the BP5/BP20 tungsten-rhenium thermocouple, 50 μm in diameter; its hot junction was welded in the specimen center.

In the thermal diffusivity studies, the specimens were the cylindrical plates, 11 mm in diameter. We selected the specimen height within the range of 0.8–2.2 mm. The mean square error of the absolute value measurement of the thermal diffusivity was within 3%; resolution was about 0.8%; the temperature step, about 1 K; and heating ranges, from 10 K/s to 200 K/s. To control the specimen state, we used a video camera with frame-by-frame synchronous registry of the video signal and of the temperature wave parameters.

We measured the electrical resistance by means of a standard four-probe potentiometer method in a vacuum (10^{-5} Pa) in helium atmosphere [7]. We installed the specimens, 2 × 2 × 15 mm parallelepipeds, inside the ring-shaped heater made of tungsten alloy. We measured temperature by means of the PR10/0 platinum-rhodium thermocouple (10% of Rh – 10% of Pt). We measured the distance between the potential contacts by means of a microscope-micrometer with a

Composition of the studied zirconium–niobium alloys

Alloy number	1	2	3	4	5	
Nb content, wt %	0	1	2.5	5	7.5	
Alloy number	6	7	8	9	10	11
Nb content, wt %	10	12.5	20	30	50	100

scale factor of 0.005 mm. The error of the electrical resistance, ρ, measurement was predominantly governed by the geometry factor and was within 1%. The average temperature measurement error at low and moderate temperatures was within 1% and, at high temperatures, within 1.5%.

We measured the electrical resistance of specimens nos. 3 and 10 (see the table) using the Linseis LSR-3 device, on 3 × 3 mm square cross-section specimens. We took the specimen temperature to equal the averaged value of the readings of upper and lower thermocouples pressed to its side surface by means of spring-loaded contacts. We delivered the current pulses in the process of isothermal ageing at temperatures of 293, 473, 873, 1073, and 1273 K. The heating between the isotherm temperatures was performed at the rate of 6 K/min, in a helium atmosphere.

PHASE DIAGRAM OF THE ZIRCONIUM–NIOBIUM SYSTEM

The phase diagram of the zirconium-niobium system is now investigated in detail [8, 9]. Figure 1 shows the diagram taken from the handbook [8]. Here, it follows that niobium is unrestrictedly dissoluble in the high-temperature BCC-modified zirconium (β-phase) and restrictedly soluble (below 5%) in the low-temperature CPH-modification (α-phase). Niobium reduces the temperature of the α–β-transition. The maximal solubility of Nb in α-Zr is about 1%. The minimum exists in the liquidus curve near 2013 K—close to 21.7% (mass) of Nb. At the temperature decrease, the β solid solution delaminates into two, β_{Zr} and β_{Nb}, that is, the solid solution of Nb in β-Zr and the solid solution of β-Zr in Nb. The lamination cupola top corresponds to about 1261 K and 60.6% (mass) of Nb. The monotectic reaction, $\beta_{Zr} - \beta_{Nb} + \alpha$, takes place at 883 K (893 K according to other data). The alloy system contamination with the O_2 and N_2 admixtures stabilizes the α-phase at temperatures above the monotectic and extends the two-phase $\beta_{Zr} + \beta_{Nb}$ domain.

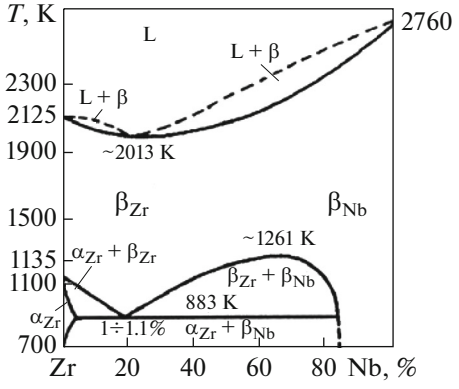

Fig. 1. Zirconium–niobium phase diagram.

EXPERIMENTAL RESULTS

Figure 2 shows the thermal diffusivity polytherms of the zirconium–niobium alloys within the temperature range of 900–1700 K. The alloys might be divided into two groups as against the character of the thermal diffusivity variation. Materials 1–6 (pure zirconium and the alloys with the niobium content within 10%) represent the first group. In the temperature dependences, $a(T)$, of these specimens, we observe, with background of general increase, a sharp value increase within the domain of polymorphous transition for the pure zirconium, no. 1 (near the temperature of 1100 K) and alloys nos. 2 and 3. This is typical for the thermal diffusivity behavior of the metals and the alloys near the structure phase transitions temperature [9]. With the niobium content increase in the alloys, the amplitude of that step decreases up to zero. In the $a(T)$ polytherms of alloys nos. 6–10, we observe monotonous thermal diffusivity increase with temperature increase.

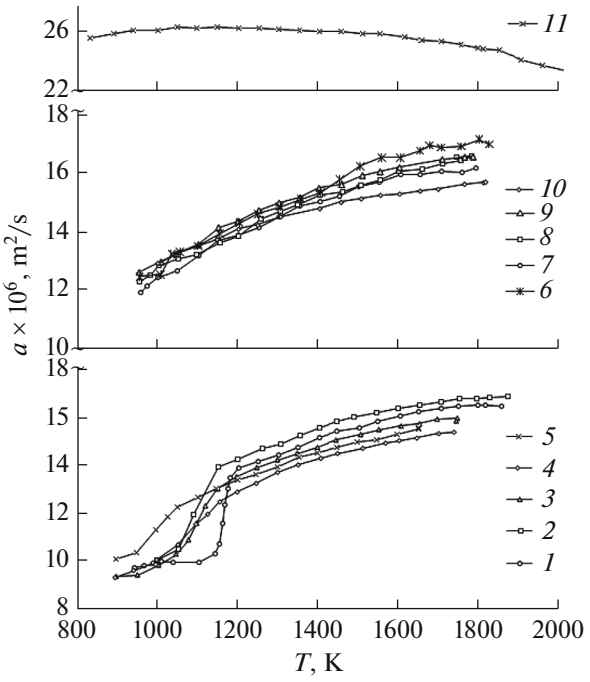

Fig. 2. Thermal diffusivity of the alloys (curve indices correpsond to the specimen numbers in the table).

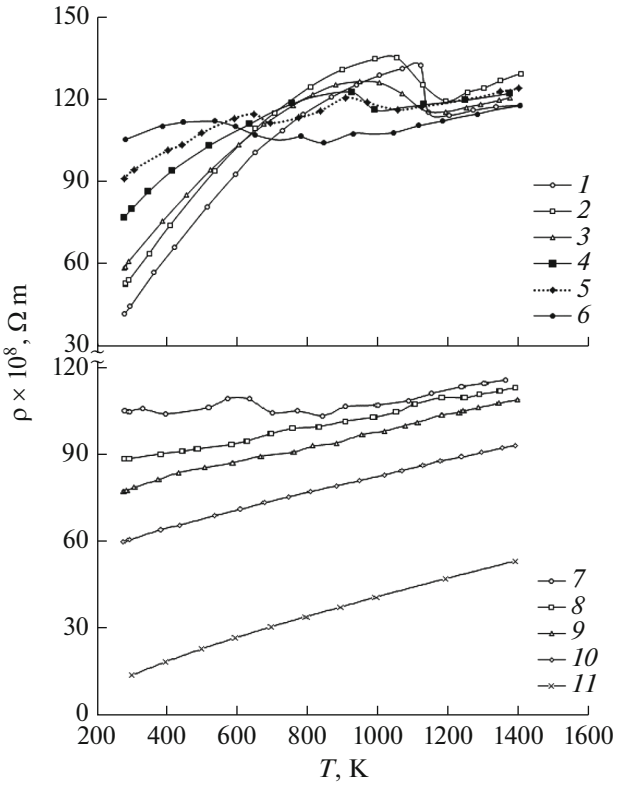

Fig. 3. Specific electrical resistivity of the alloys (curve indices correspond to the specimen numbers in the table).

The polytherm, $a(T)$, no. 11 for the pure niobium is distinguished by higher thermal diffusivity values (as against the alloys) and by the character of its variation with the temperature increase. First, the thermal conductivity slightly increases and then monotonously decreases.

Figure 3 shows the polytherms of the specific electrical resistivity of the studied alloys within the temperature range of 300–1500 K. Note that, for the alloys 1–7, the polymorphous transition is characterized by the wave-like domain in all the temperature dependences, $\rho(T)$,—that fact is in good agreement with the state diagram. Within the considered temperature range, with temperature increase, the specific electrical resistivity of the studied alloys increases or remains in fact invariable. The experimental data obtained at the different facilities coincide within experimental error.

Note the following peculiarities of the physical characteristics of the alloys. Within the iso-structure state domain, the thermal diffusivity and the specific electrical resistivity increase with the temperature increase. For the specific electrical resistivity, this increase is characterized by the negative curvature. The thermal diffusivity and the specific electrical resistivity of niobium differ essentially from the properties of zirconium and the alloys in its values and the character of variation under heating.

DISCUSSION

The problem of mechanisms providing the general energy transfer through the studied alloys is of primary interest. Two such mechanisms are known [10] in the metal substances at high temperatures: the electron and the phonon. We might estimate the electron contribution according to the Wiedemann–Franz law [10]. Thus, according to the thermal diffusivity definition [11], we calculate the general thermal conductivities, $\lambda(T)$, of the alloys. Here, we engaged the data on the heat capacity and the density obtained by means of the percent recalculation for the pure substances [11] (without account for the temperature variations of the density).

Figure 4 shows the results of the $\lambda(T)$ calculations in solid lines. Note that the thermal properties—in particular, the thermal conductivity—of the pure zirconium and niobium as well as of certain alloys were investigated earlier. Figure 4 shows some of these data in hatch lines. Here, for the pure zirconium and niobium, we show the reference data [11]; for the alloy no. 2—the data [12]; for the alloy no. 3—[13]. From Fig. 4, it follows that the present results and the literature data are in satisfactory agreement.

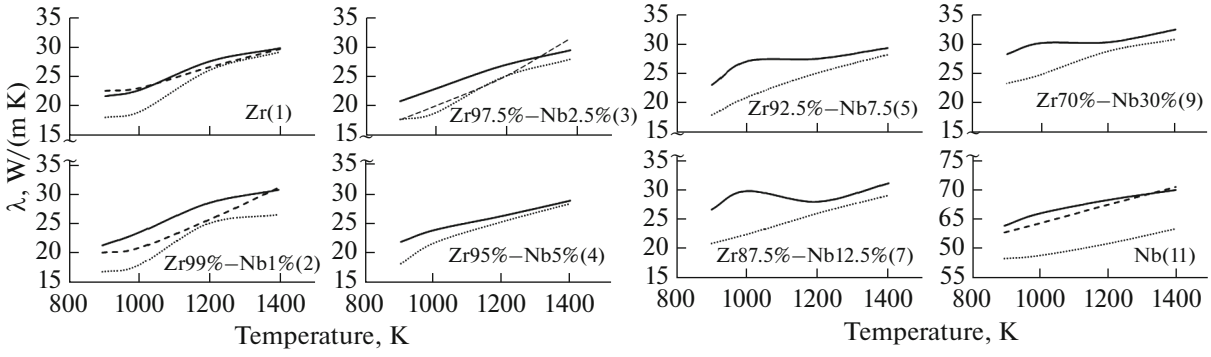

Fig. 4. Thermal conductivity of the alloys (component concentration corresponds to the table).

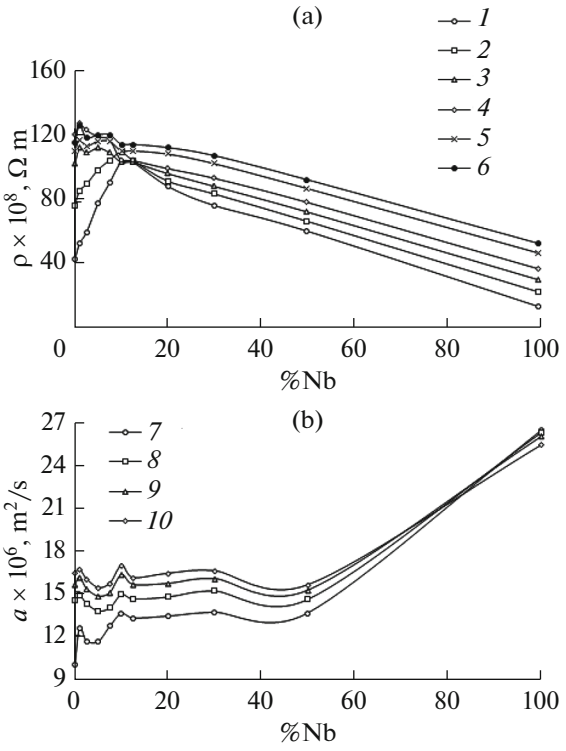

Fig. 5. Concentration dependences of specific electrical resistivity (a) and thermal diffusivity (b): *1*—300 K, *2*—500 K, *3*—700 K, *4*—900 K, *5*—1200 K, *6*—1400 K, *7*—1100 K, *8*—1300 K, *9*—1500 K, *10*—1700 K.

We calculate the electron constituents of the thermal conductivity, $\lambda_e(T)$, according to the Wiedemann–Franz law, on the basis of our data on the specific electrical resistivity (see Fig. 3). These calculation results are also present in Fig. 4 in dotted lines.

From the comparison of $\lambda(T)$ and $\lambda_e(T)$, it follows that the electron mechanism of the energy transfer is the main one in the considered substances. This conclusion is in agreement with [12, 13]. The predominant role of the electron mechanism makes it possible to analyze the electrical resistance and the heat transfer characteristics in common, on the basis of the properties of collectivized electrons in given substances.

Consider temperature dependences of the studied properties. From the results presented in Figs. 2–4, it follows that all the kinetic characteristics of the alloys either increase or do not decrease at heating. The character of variation of the kinetic characteristics of the alloys as well as of the pure zirconium and niobium are evidence of the multiband conductivity of these objects [10]. The level of the chemical potential of zirconium is located at the rise of the density of state function of the collectivized electrons—within the domain with high value of the *d*-electron density whereas that of niobium is located at the density of state decline—in the domain with low density of the *d*-electron state [14–16]. The properties of these alloys reflect that fact.

The polytherms of the specific electrical resistivity of zirconium and the alloys with low niobium content are characterized by pronounced negative curvature (Fig. 3) because the chemical potential level decreases with heating—similar phenomenon takes place for rareearth metals [17]. Decrease of the scattering process intensity is a consequence of that decrease and results in deceleration of the specific electrical resistivity increase and the increase of electron thermal conductivity under heating. The calculation shows that the electron constituent of the thermal conductivity dominates in those alloys. That is why the temperature dependence of the total thermal conductivity is also nondecreasing (Fig. 4). The considered effects take place also in the other alloys with higher niobium content; yet, they are less pronounced.

Consideration of the CPH–BCC phase transition within the framework of the presented model gives rise to the conclusion that, in the BCC phase, the density of state of the *d*-electrons in zirconium turns out to be lower than the same in the CPH phase. At the expense of that process, anomalous decrease of the specific electrical resistivity (Fig. 3) and an increase of the thermal diffusivity (Fig. 2) take place. As usual, admixture injection results in widening of the temperature interval where the phase transition takes place. The average temperature of the phase transition decreases—in agreement with the phase diagram (Fig. 1). Anomalous variation of the kinetic properties of the alloys with high niobium content (10% (mass) and higher) in the vicinity of the CPH–BCC transition becomes in fact imperceptible.

Consider the concentration dependence shown in Figure 5 for the specific electrical resistivity and the thermal diffusivity. Note that these alloys form the solid solution system only at high temperatures when the substance is in the BCC phase. At lower temperatures, the phase composition of the alloys becomes nonuniform. This fact makes it difficult to analyze obtained results from the united standpoint within the whole range of the studied temperatures.

At 300 K, with the Nb concentration increase, strong electric resistivity increase from 40×10^{-8} to 110×10^{-8} Ω m takes place. At the Nb content of 10%, the specific electrical resistivity reaches its maximum. We observe certain similarity of the cupola-like dependence reminiscent of the Nordheim rule [10], although, in general, it is not valid for the given alloys. With further temperature increase (that is, ≥700 K), the specific electrical resistivity of the alloys varies, with the concentration increase, more smoothly, the intensity of the maximum decreases and shifts to the lower Nb concentration domain.

Note that the peculiarities of the electron and the phonon structures of the alloys are not discovered within the studied temperature range. Yet, we might

suppose that the above peculiarities are related to the properties of the collectivized electrons. Zirconium and niobium are neighbors in D.I. Mendeleev's periodical table and their atomic masses are close to each other. Thus, the additional scattering mechanisms occurring with the admixture injection are related with the properties of the collectivized electrons. Accounting the fact that both alloy components are transition metals, we connect the observed phenomena with the concentration variations of the state densities of the alloys. Detailed analysis of a similar situation is presented in [18, 19]. That analysis gives rise to the supposition that, in the CPH phase, the niobium admixture injection to zirconium results in noticeable scattering increase (that is, the electrical resistance increase) caused by the increase of the density of state of the *d*-electrons in the alloys. The density of state value reaches its maximum near the 10% (mass) of niobium. It is due to this effect that the maximum of the specific electrical resistivity is observed in the concentration dependence for 300 K (Fig. 5a).

Under heating, the substance transits into the solid solution state (the BCC phase). The experiment shows that the situation varies. The electrical resistance increase at the expense of the niobium admixture injection becomes less noticeable. In fact, monotonous decrease in the specific electrical resistivity takes place with niobium concentration increase (Fig. 5a). The cupola of the concentration dependence of the electrical resistance shifts to the low concentrations and becomes less pronounced (Fig. 5a, curves *5* and *6*). In fact, the concentration dependences little by little degenerate into the straight lines connecting the characteristic values for pure metals. The concentration dependences of the thermal diffusivity (Fig. 5b) behave qualitatively similarly (note that the thermal characteristics describe the properties of not only the electrons but also the lattice). Their shape is the same at all the temperatures. In the isotherms, we observe two moderate maximums at the niobium concentrations of 1% and 10%. At the niobium concentrations from 20% to 50%, the thermal diffusivity varies insufficiently.

Such type dependence is evidence of the fact that, in the solid solutions, the niobium concentration variation results in a decrease of the *d*-electron density of state; yet, this variation is smoother than the same at low temperatures. The electron density of state does not undergo sharp variations.

The thermophysical characteristics also show a dependence on the structure of the Zr–Nb alloys. This problem is considered in [20].

CONCLUSIONS

(1) As the result of the performed investigations, we obtain data on the thermal diffusivity and the electrical resistance of the double Zr–Nb system. In the polytherms of the physical properties, within the structure phase transition domains, at low niobium concentrations, we observe anomalous variations in the form of steps.

(2) The concentration dependences of the properties obtained in the present work are characterized by consistency; yet, the character of their variations differs from the Nordheim rule [10].

(3) The temperature dependences of the kinetic characteristics of the zirconium–niobium alloys at high temperatures, within the domains of iso-structure state, are monotonous functions of temperature. The specific electrical resistivities of the alloys are described by the dependences with the negative curvature. The thermal diffusivity and the thermal conductivity polytherms are nondecreasing.

(4) The main variation peculiarities of the kinetic characteristics of the zirconium–niobium alloys might be explained by the electron multiband conductivity.

ACKNOWLEDGMENTS

The work was supported by the Russian Foundation for Basic Research, project nos. 11-08-00275 and 14-08-00228.

REFERENCES

1. Kalin, B.A., Platonov, P.A., Chernov, I.I., and Shtrombakh, Ya.I., *Fizicheskoe materialovedenie. Uchebnik dlya vuzov* (Physical Materials Science. Textbook for High Schools), 6 vols., Kalin, B.A., Ed., vol. 6, part 1: *Konstruktsionnye materialy yadernoi tekhniki* (Structural Materials in Nuclear Engineering), Moscow: MIFI, 2008.
2. *Thermophysical Properties of Materials For Nuclear Engineering: A Tutorial and Collection of Data*, Vienna: IAEA, 2008.
3. Chirkin, V.S., *Teplofizicheskie svoistva materialov yadernoi tekhniki* (Thermal Properties of Materials of Nuclear Engineering), Moscow: Atomizdat, 1967.
4. Onufriev, S.V., Kondratiev, A.M., Savvatimskiy, A.I., Val'yano, G.E., and Muboyajan, S.A., *High Temp.*, 2015, vol. 53, no. 3, p. 455.
5. Gorbatov, V.I., Il'inykh, S.A., Taluts, S.G., and Zinov'ev, V.E., *Inzh.-Fiz. Zh.*, 1988, vol. 55, no. 3, p. 485.
6. Ivliyev, A.D., *High Temp.*, 2009, vol. 47, no. 5, p. 737.
7. Peletskii, V.E., Timrot, D.L., and Voskresenskii, V.Yu., *Vysokotemperaturnye issledovaniya teplo- i elektroprovodnosti tverdykh tel* (High-Temperature Studies of Thermal and Electrical Conductivity of Solids), Moscow: Energiya, 1971.
8. *Diagrammy sostoyaniya dvoinykh metallicheskikh sistem. Spravochnik* (Diagrams of Binary Metallic Systems: Reference Book), 3 vols., Lyakishev, N.P., Eds., Moscow: Mashinostroenie, 2001, vol. 1.
9. *Waterside Corrosion of Zirconium Alloys in Nuclear Power Plants*, Cox, B., Kritsky, V.G., Lemaignan, C., Eds., Vienna: IAEA, 1998.
10. Ziman, J.M., *Electrons and Phonons*, Oxford: Clarendon Press, 1960.

11. Zinov'ev, V.E., *Teplofizicheskie svoistva metallov pri vysokikh temperaturakh* (Thermal Properties of Metals at High Temperatures), Moscow: Metallurgiya, 1989.
12. Peletskii, V.E., Grishchuk, A.P., and Musaeva, Z.A., *Teplofiz. Vys. Temp.*, 1994, vol. 32, no. 6, p. 820.
13. Musaeva, Z.A. and Peletskii, V.E., *Teplofiz. Vys. Temp.*, 2005, vol. 43, no. 5, p. 697.
14. Bakonyi, I., Ebert, H., and Liechtenstein, A.I., *Phys. Rev. B: Condens. Matter Mater. Phys.*, 1993, vol. 48, no. 11, p. 7841.
15. Grad, G.B., Blaha, P., Luitz, J., Schwarz, K., Fernández, G.A., and Sferco, S.J., *Phys. Rev. B: Condens. Matter Mater. Phys.*, 2000, vol. 62, no. 19, p. 12744.
16. Irkhin, V.Yu. and Irkhin, Yu.P., *Elektronnaya struktura, fizicheskie svoistva i korrelyatsionnye effekty v d- i f-metallakh i ikh soedineniyakh* (Electronic Structure, Physical Properties and Correlation Effects in *d*- and *f*-Metals and Their Compounds), Yekaterinburg: Uralsk. Otd. Ross. Akad. Nauk, 2004.
17. Ivliev, A.D., *Fiz. Met. Metalloved.*, 1993, vol. 75, no. 2, p. 9.
18. Tsiovkin, Yu.Yu., Vishnekov, L.Yu., and Voloshinskii, A.N., *Fiz. Met. Metalloved.*, 1991, no. 7, p. 48.
19. Tsiovkin, Yu.Yu., Vishnekov, L.Yu., and Voloshinskii, A.N., *Fiz. Met. Metalloved.*, 1991, no. 8, p. 76.
20. Gorbatov, V.I., Polev, V.F., Korshunov, I.G., Pilyugin, V.P., Smirnov, A.L., and Taluts, S.G., *High Temp.*, 2016, vol. 54, no. 2, p. 294.

Translated by I. Dikhter